High energy ($E \leq 1000$ GeV) intranuclear cascade model for nucleons and pions incident on nuclei and comparisons with experimental data*

H. W. Bertini,† A. H. Culkowski,‡ O. W. Hermann,‡ N. B. Gove,‡ and M. P. Guthrie†
Oak Ridge National Laboratory, Oak Ridge, Tennessee 37830
(Received 18 August 1977)

An intranuclear cascade model for reactions of pions and nucleons with complex nuclei that should cover the energy range from about 50 MeV to about 1000 GeV has been developed. The model includes the effect of a diffuse nuclear surface, the Fermi motion of the bound nucleons within the nucleus, the exclusion principle, a local potential for nucleons, a localized reduction in the density of the nucleus during the development of the cascade, and the sequencing of the events correctly with time. Theoretical results from the model are compared with experimental data over the energy range ~3–1000 GeV. Within the cascade model, the equations that are used to represent the pion multiplicity from the reactions of nucleons and pions with the individual nucleons of the nucleus underestimates the number of shower particles produced by these individual nucleon interactions. In spite of this the predicted number of shower particles escaping from the nucleus, for 100-GeV nuclear interactions, is overestimated by about 25% for light nuclei to about 60% for heavy nuclei. The agreement for the number of escapes from the nucleus is somewhat better at lower interaction energies (~10–20 GeV). Some of the major trends in the observed high energy data are predicted quite well. These include the energy independence of (a) the number of black tracks produced at interaction energies above 5 GeV, (b) the number of shower particles produced above 100 GeV, and (c) the radionuclides produced above 10 GeV. Other trends that are predicted fairly well are the small mass dependence of the shower particle multiplicity (factor of 2 increase predicted from carbon to lead; factor of 1.5 measured), and the change in the angular dependence of the multiplicity with mass. In absolute comparisons, the predicted total reaction cross sections are in good agreement with experimental data, and the cross sections for the production of radionuclides are in fair agreement.

[NUCLEAR REACTIONS Theoretical, intranuclear cascade method, $\sigma_t(A)$ for p and π, $\langle n\rangle_{\text{shower}}$ and $\langle n\rangle_{\text{black}}$ vs E_π, $\sigma(\theta_\pi)\Delta\theta_\pi$ vs A, $\sigma(E_\pi, E_p{:}\theta)$ for p on Al, radiochemical σ's for 11- and 300-GeV p on ^{59}Co. All compared with experiment.]

INTRODUCTION

The interaction of nucleons and π-mesons at high energies (~100 GeV) with nuclei is calculated using the intranuclear cascade approach with a computer program called HECC-1. In this approach the transitions to the continuum states of the final residual nuclei from the interaction of a high-energy particle with a target nucleus is determined by calculating the individual life histories of the incident particle, and all subsequent collision products, as they travel through the nucleus and interact with the bound nucleons therein. A cascade of particles is thus generated within the nucleus. The interactions with the bound nucleons are considered to be free-particle interactions modified by exclusion effects. These free-particle reactions include scattering, charge exchange scattering (for π-nucleon reactions), production of π-mesons, and pion absorption.[1] Monte Carlo techniques are used to specify all of the variables needed to determine the life histories. The nucleus is left in a highly excited state after the completion of the cascade, and an evaporation calculation is employed to permit the deexcitation of the nucleus.[2]

The method differs from that reported previously[3,4] in that the cascade events that are assumed to occur inside the nucleus are properly sequenced in time whereas in the previous work this was not the case, and the local nuclear density in the vicinity of a cascade collision is reduced to account for the removal of a nucleon from the Fermi sea. In the earlier work the reduction of the nuclear density as the cascade developed was ignored.

Various trends in the interaction of high-energy nucleons and pions with nuclei have been discerned and summarized recently,[5] and the ability of the model to predict these trends along with other comparisons with experimental data will be examined. All of the calculated results shown below are in absolute units unless specified otherwise.

OTHER APPROACHES

Other approaches in the calculation of very high-energy nuclear reactions are under study. One is the multiperipheral model[6] in which a series of particles of decreasing rapidity {the rapidity $y = \frac{1}{2}\ln[(E+p_z)/(E-p_z)]$} are emitted until a parti-

cle with rapidity equal to that of the target interacts with the target. Given a characteristic time T_0, in the rest frame of the particle, it is assumed that only those particles can interact with the nucleons of the nucleus if in time T_0 they have not passed the nucleus. Thus, only the last of the particles in the emitting chain can interact with the nucleus. The effect of the model is to enhance the rapidity distribution for a nuclear reaction, compared with that for hadron-hadron reactions, only at the low end of the rapidity scale. This is in conformity with some of the broad features of the experimental data.[5]

Another model that qualitatively yields the same rapidity distribution is the energy flux cascade model.[7] A hadron-nucleon collision within the nucleus is assumed to form an excited hadronic state, the energy flux, which instantaneously acquires a rapidity distribution that is the same as the asymptotic distribution of produced particles in a hadron-hadron collision. As time proceeds the distribution spreads out in space with the faster part of the distribution in the front and the slower part at the end. When any part of the distribution reaches a spatial size equal to that of a single hadron, it behaves as a single hadron with a rapidity equal to the average rapidity of that part of the distribution. In approximately one mean free path within the nucleus the front part of the distribution has sufficiently spread to be considered as a single hadron which interacts with another nucleon. The remaining part has a lower energy, and it produces negligible multiplicity upon interacting with a nucleon. The process continues in this manner with new energy flux created at the end of each mean free path.

Another approach is the conglomerate model[8] in which it is assumed that the interaction time is so long that all of the nucleons in the path of the incident particle are involved as a conglomerate which decays outside of or independently of the nucleons remaining. This will move the tailing end of the rapidity distribution backward in the lab frame, which again roughly corresponds to the observed data.

The last model to be discussed is an intranuclear cascade calculation developed by Artykov *et al.*[9] In this version the nucleons in the nucleus are assigned fixed locations within the nucleus, and they are distributed such that their density is uniform throughout the nucleus. The nucleus is given a random rotation for the calculation of each incident particle. During the calculation of the cascade, when the trajectories of more than one cascade particle terminate at or near the position of a fixed nucleon within the nucleus, these cascade particles all interact simultaneously with the single fixed nucleon (many-particle interaction). Although fixed in space the struck nucleon is allowed to have a momentum governed by a zero temperature Fermi distribution. The energy available to produce pions from this many-particle interaction is the "free energy" ϵ where

$$\epsilon = \left[\left(\sum_i E_i \right)^2 - \left(\sum_i \vec{p}_i \right)^2 \right]^{1/2} - \sum_i m_i$$

with E, p, and m representing the total energy, momentum, and mass of the particles involved. The energy and angular distrubution of the secondary particles are taken from the energy-dependent experimental data of secondary particles produced from nucleon-nucleon reactions.

When only one cascade trajectory terminates in the vicinity of a fixed nucleon, the reaction is calculated as a free-particle reaction where scattering and pion-production reactions are included. In all cases exclusion effects are included, and also calculations were carried out with and without the effects of a "leader" particle, i.e., a single particle that carries off most (50–70%) of the available energy. Those fixed nucleons that are struck are removed from the sea of fixed nucleons and hence a local void is created.

Comparisons with experimental data indicate that the leader particle, when employed, creates an excessive number of shower particles at reaction energies of ~100 GeV. At lower energies ($E \leq 30$ GeV) only small differences in results with or without it are ascertained. A better agreement with experimental data is obtained when many-particle interactions are included.

The intranuclear cascade model described in this paper differs in that no multiparticle reactions are considered and effects of a leader particle are not included. The time sequence of events is taken into account whereas it is not by Artykov *et al.*, and both include the effects of the reduction of nuclear density at each interaction site within the nucleus.

MODEL OF THE NUCLEUS

Detailed descriptions of the properties of the nucleus that are taken into account are given elsewhere.[3,10] Changes from the earlier versions that have been incorporated will be described in some detail. The model nucleus can be divided into a maximum of 50 spherical annuli. Each annulus can further be divided by 50 planes all intersecting along the z axis and equally spaced from each other in angle, and 50 cones that originate at the origin and for which the z axis is the axis of symmetry. Each annulus can be subdivided into planes and cones independently of the other annuli. How-

ever, the memory space within the computer program that is allocated to carry all of the information required for the cascade-particle histories would probably be exceeded if the maximum numbers of subdivisions were used. In our experience the program will accommodate a total of 300 subdivisions (regions) of the nucleus without exceeding the cascade-particle memory requirements. All regions within a spherical annulus have the same density, but the density decreases from annulus to annulus from the center to the outer boundary.[10]

The effects of a spatially dependent potential are included for nucleons,[10] but not for pions. The Fermi motion of the bound nucleons and the effects of the exclusion principle are taken into account.[3,10] Reflection and refraction[11] and nuclear correlations[12] are not included. The latter is included only in that pion absorption is assumed to take place with nucleon-nucleon pairs within the nucleus.[10]

The sampling technique that was used to select the momentum of the struck nucleon is described in another report[13] as is the method for determining the relative probabilities of nucleon and pion collisions. Also included is the method for determining the type of collision, i.e., scattering, charge exchange scattering, pion production, etc.

PARTICLE-PARTICLE INPUT DATA

All nucleon-nucleon cross sections at energies below 3.5 GeV and all pion-nucleon cross sections at energies below 2.5 GeV were taken to be the same as those used in the lower energy version

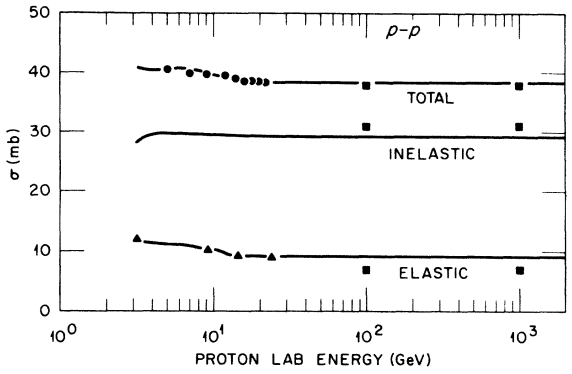

FIG. 1. High-energy p-p cross sections. Solid lines are the cross sections used in the calculation. ●: W. Galbraith *et al.*, Phys. Rev. 138, B913 (1965); ■: L. V. Vokova, Izv. Akad. Nauk SSSR-Ser. Phys. 31, 1472 (1967) [Bull. Acad. Sci. USSR, Phys. Series 31, 1508 (1967)] (theoretical prediction); ▲: G. Alexander *et al.*, Nucl. Phys. B5, 1 (1965). When not shown, experimental error bars are smaller than the symbols.

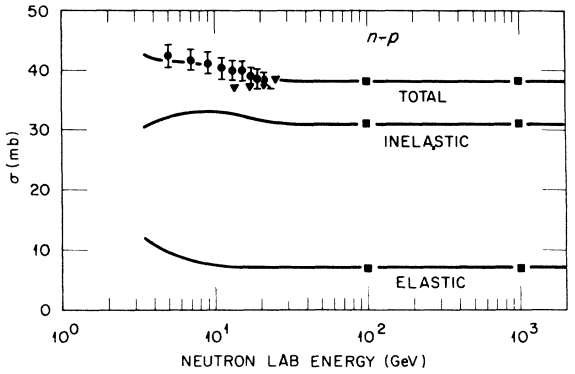

FIG. 2. High-energy n-p cross sections. ▼ M. N. Kreisler *et al.*, Phys. Rev. Lett. 20, 468 (1968). All else as in Fig. 1.

of the calculation (MECC-7).[4] At higher energies the particle-particle cross sections that were used are illustrated in Fig. 1–4. The n-n cross section was taken to be the same as the p-p cross section; the π^--n cross section was set equal to the π^+-p cross section, and the $\pi^\pm$-n, π^0-n, and π^0-p cross sections were arbitrarily set equal to the π^--p cross section. These assignments apply for the differential cross sections as well.

The differential scattering cross section for particle-nucleon scattering at energies greater than 3.5 GeV for incident nucleons and at energies greater than 2.5 GeV for incident pions was represented by

$$\frac{d\sigma}{dt} = \exp(A - B|t|),$$

where t is the square of the four-momentum transfer in the center of momentum (c.m.) system, and it is related to the scattering angle in this system by

$$\cos\theta_{\text{c.m.}} = 1 - \frac{|t|}{2K^2}.$$

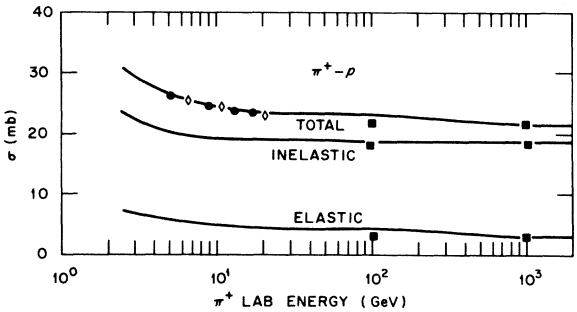

FIG. 3. High-energy $\pi^+ + p$ cross sections. ◇ K. J. Foley *et al.*, Phys. Rev. Lett. 19, 330 (1967). All else as in Fig. 1.

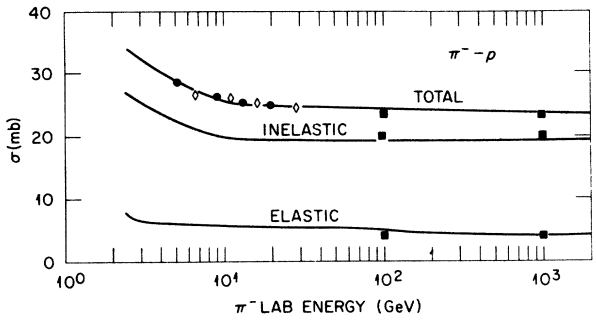

FIG. 4. High-energy $\pi^- + p$ cross sections. Symbols defined in Figs. 1 and 3.

K^2 is the square of the three-momentum of either particle in the c.m. system before or after scattering with

$$K^2 = \frac{M^4 - 2M^2(m_1^2 + m_2^2) + (m_1^2 - m_2^2)^2}{4M^2},$$

where M is the total energy in the c.m. system and m_1 and m_2 are the rest masses of the particles involved in the collision. The constant A was used only for normalization purposes. For nucleon-nucleon scattering the parameter B was taken to be

$$B = 7.26 + 0.0313 p_0,$$

where p_0 is the momentum of the incident particle. This representation of the parameter B compared with the values obtained when experimental cross section data[14] were fitted by $d\sigma/dt = \exp[A - B|t|]$ are shown in Fig. 5.

For $\pi^+ - p$ and $\pi^- - p$ scattering the values of B were taken to be constant at 7.575 and 7.04, respectively. These are the average values of those reported in Ref. 15 which were obtained by fitting experimental data over the energy range from 8.5 to 18.4 GeV/c.

The sampling technique that was used to specify the scattering angles in the c.m. system is described elsewhere.[16]

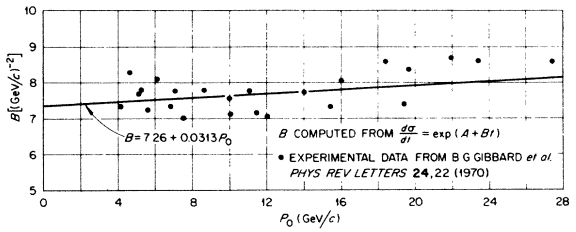

FIG. 5. Parameter B for the differential nucleon-nucleon scattering cross section vs the momentum of the incident particle in the lab system.

CALCULATION

Since adequate descriptions of the general approach to the calculation of nuclear reactions by the method of intranuclear cascades have appeared in the literature,[1,9-13] only those features of the calculation that are different from the version that applies at lower energies[4] will be described here.

Time sequence of events

One of the features of the present model that is different from the intranuclear cascade model reported previously[3,4] is that the cascade events are properly sequenced in time. The time t is set to zero when the incident particle has made a collision. Two time values are associated with every particle that makes up the cascade. One is the time at which the particle will make the next collision, t_c, and the other is the time that the particle will cross the boundary of the region in which it is located, t_b. Both t_c and t_b are measured from $t = 0$, when the cascade was initiated. The time-to-the-boundary crossing is calculated as though no collision were scheduled to take place within the region. Whether this will be true or not depends on whether the sampled site of the next collision lies outside or inside of the region. The time between events (either boundary crossings or collisions) is calculated by dividing the distance between them by the velocity of the particle. The next event, out of all possible events, is determined by the smallest value of all of the listed t_b's and t_c's.

It was necessary to include boundary crossings as events so that an account of the effect of a reduction of the density in the regions that lie in the paths of the cascade particles could be made. In other words, if the density of a region were reduced because of a collision that took place within it at an earlier time, then this reduced density would be used to determine the collision probability within that region for cascade particles that arrived at a later time. When a particle arrives at a boundary, the density of the region that the particle is about to enter is examined to see if it has been reduced. If it has not, the calculation proceeds, and if it has, a new probability for a collision within the region is calculated.

Density depletion

Each incident particle interacts with an undisturbed nucleus whose density is normalized such that

$$\int (\rho_p + \rho_n) dV = \sum_{i=1}^{R} (\rho_{pi} + \rho_{ni}) V_i = A,$$

where ρ_p and ρ_n are the number of protons and

neutrons per cm^3; the subscript i refers to the ith region number; R is the number of regions in the nucleus; and A is the mass number of the nucleus. If a collision in the ith region occurs with a proton (similarly with a neutron), the density in that region is reduced by one proton, i.e.,

$$\Delta\rho_{pi}V_i = 1 ,$$

and the residual density ρ^r_{pi} is given by

$$\rho^r_{pi} = \rho_{pi} - \Delta\rho_{pi} .$$

If the residual density is less than zero, the density in that region is set equal to zero, and nuclear matter is subtracted from the nearest-neighbor regions in such a manner that the total reduction in nuclear matter is equal to one proton. This is accomplished by reducing the density of the ith nearest-neighbor region by an amount $\Delta\rho_{pj}$ such that

$$V_j\Delta\rho_{pj} = \frac{\rho_{pj}V_j(1-\rho_{pi}V_i)}{\sum_{j=1}^{n}\rho_{pj}V_j} ,$$

where n is the total number of nearest-neighbor regions. If the residual densities of the nearest-neighbor regions are less than zero, their densities are set equal to zero and the deficit in nuclear matter that must be made up to equal one proton is subtracted from the next-nearest neighbors in a similar matter.

This procedure is adopted to insure that the depletion of the nuclear matter is localized or centered at the location at which the collision occurred. Nearest-neighbor regions are those that have a bounding surface that partially or completely overlaps a surface of the region in question, and next-nearest neighbors are those whose corners (loosely speaking) touch the corners of the region.

Multiple particle production

At the lower energies ($E \leq 2.5$ GeV for pions and ≤ 3.5 GeV for nucleons) the production of pions in particle-particle reactions is treated in the same manner as was done previously,[3,4] i.e., the Lindenbaum Sternheimer isobar model was employed.[17] At higher energies the empirical formulas developed by Ranft were employed to determine the multiplicities and the spectra of the secondary particles.[18] The creation of all particles other than pions was ignored mainly because pion production is by far the dominant mode.

Given that a collision has taken place, the equation that describes the nucleon spectra from inelastic nucleon-nucleon collisions for a system in which the struck nucleon is at rest is

$$N_{nn}(p,\theta) = \left(\frac{A}{p_0}+\frac{Bp}{p_0^2}\left\{1+\left[1+\left(\frac{p_0}{m}\right)^2\right]^{1/2}-\frac{p_0}{p}\left[1+\left(\frac{p}{m}\right)^2\right]^{1/2}\right\}\right)$$
$$\times p^2\left\{1+\left[1+\left(\frac{p_0}{m}\right)^2\right]^{1/2}-\frac{pp_0}{m^2}\left[1+\left(\frac{p}{m}\right)^2\right]^{-1/2}\right\}\exp(-cp^2\theta^2) , \quad (1)$$

where $N_{nn}(p,\theta)$ is the number of nucleons per unit momentum per unit solid angle; p is the momentum in GeV/c of the secondary nucleons; p_0 is the momentum of the incident nucleon (GeV/c); m is the rest mass of the nucleon (GeV); θ is the polar angle of the secondary particle (rad); $A = 0.55$; $B = -0.30$; and $C = 2.68$.

The equation for the secondary pion spectra in a nucleon-nucleon collision is

$$N_{n\pi}(p,\theta) = A_1p^2\exp(-A_2pp_0^{-1/2}-A_3pp_0^{1/2}\theta^2)$$
$$+(B_1p^2/p_0)\exp[-B_2(p/p_0)^2-B_3p\theta] , \quad (2)$$

where p is the momentum (GeV/c) of the secondary pion, p_0 the momentum of the incident nucleon, and the constants are taken to be

$$A_1 = 4.75 , \quad B_1 = 3.546 ,$$
$$A_2 = 3.76 , \quad B_2 = 10.21 ,$$
$$A_3 = 4.23 , \quad B_3 = 4.28 .$$

The normalization of this expression is such that integration over all angles and all secondary particle momentum will give the total pion multiplicity (i.e., the sum of the numbers of secondary π^+, π^0, and π^-) for an incident nucleon with momentum p_0. It was arbitrarily assumed that the multiplicity of pions of each charge state was $\frac{1}{3}$ the total.

Equations (1) and (2) were found to fit experimental data reasonably well.[19] Equation (2) was arbitrarily used to represent the recoil nucleon and the secondary pion spectra from pion-nucleon inelastic collisions by letting p_0 represent the momentum of the incident pion and p the momentum of the recoil nucleon or the secondary pion. Although a renormalization would appear appropriate to account for the phase space differences when Eq. (2) is applied to the two different reactions, such a renormalization would not affect the results. The reason is that all of the distributions are renormalized to unity anyway in order to make

use of the Monte Carlo sampling techniques.

A detailed description of the Monte Carlo sampling technique that is employed for these distribution functions is given elsewhere.[16] The technique is such that total energy, charge, and baryon number (nucleons in this case) are conserved for each of the individual particle-particle interactions; momentum is not conserved. Momentum is not conserved in the method of sampling because the information included in the distributions is insufficient for the complete specification of all possible reactions. Unless the dynamics of the reaction are described strictly by statistical theory, an essentially complete specification is required in order to sample in such a way that both energy *and* momentum are conserved. The secondary particle spectra in these inelastic collisions are determined in the system in which the struck particle is at rest. Momentum nonconservation in this system results in energy nonconservation in the laboratory system when the usual relativistic transformations to the laboratory system are made. Conservation of energy in the lab system is imposed by renormalizing, i.e., following the transformation to the lab system, the transformed energy of each particle is multiplied by the ratio of the initial total laboratory energy of the reaction to the sum of the total energies of all of the particles following the transformation. The magnitude of the momentum of each particle is recalculated to correspond to the renormalized total energy of the particle, but its direction cosines are unchanged from those obtained from the transformation.

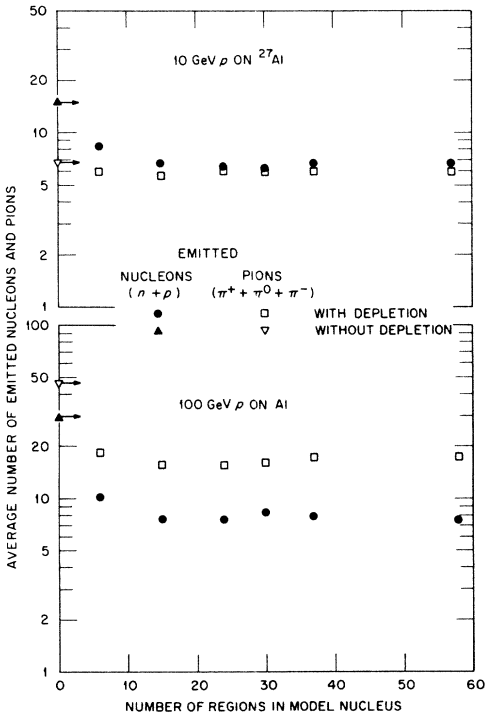

FIG. 6. Average number of emitted nucleons $(n+p)$ and pions $(\pi^+ + \pi^0 + \pi^-)$ per incident particle collisions vs the number of regions used in the model nucleus. The reactions are 10- and 100-GeV p on ^{27}Al. The results for the cases without the inclusion of nuclear density depletion are independent of the number of regions (indicated by the arrows). The statistical error associated with each data point is about the size of the symbol.

EFFECT OF DENSITY DEPLETION AND NUMBER OF REGIONS

The effects on the secondary particle multiplicities of the number of regions used in the calculation, and the effects of nuclear density depletion are illustrated in Figs. 6 and 7. The particle multiplicities are independent of the number of regions used in the model nucleus beyond about 15 regions for Al and 50 regions for Pb. When the number of regions is greater than these values the deviations from a straight line are within the statistics of the results. When nuclear density depletion is not taken into account the effect on the nucleon multiplicity is large at all energies shown, but it is large for the pion multiplicity only at the

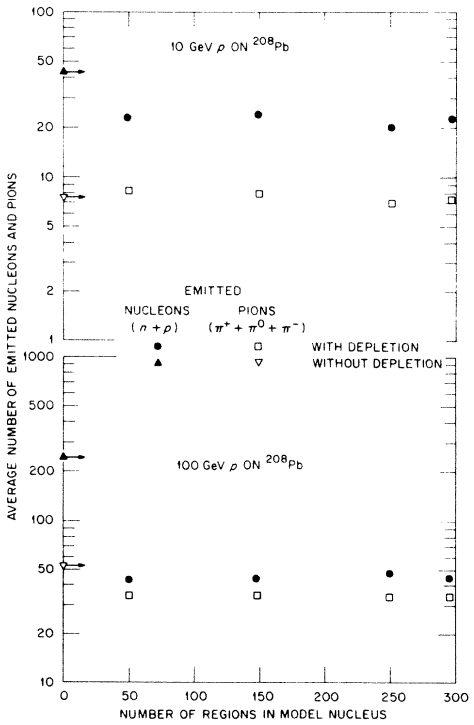

FIG. 7. Same as Fig. 6 for the reactions of 10- and 100-GeV p on ^{238}U.

higher energies. Results for the cases without depletion are independent of the number of regions.

For all of the comparisons illustrated below the number of regions for each target nucleus was taken to be approximately equal to the mass number of the target, and nuclear depletion was included.

COMPARISONS WITH EXPERIMENTAL DATA

Total nonelastic cross sections

Comparisons of the theoretical predictions with the experimental data for ~50-GeV pions and protons on various targets are shown in Fig. 8. The agreement is quite good.

Particle multiplicities

Comparisons between theoretical predictions and experimental data for the secondary particle multiplicities have been made on an absolute basis, i.e., comparing absolute numbers of particles produced from the reactions, and on a relative basis, i.e., comparing ratios of particles produced from the nuclear reactions to numbers of particles produced from p-p reactions.

Absolute multiplicities

Figure 9 illustrates comparisons between experimental emulsion data[20] and predictions from

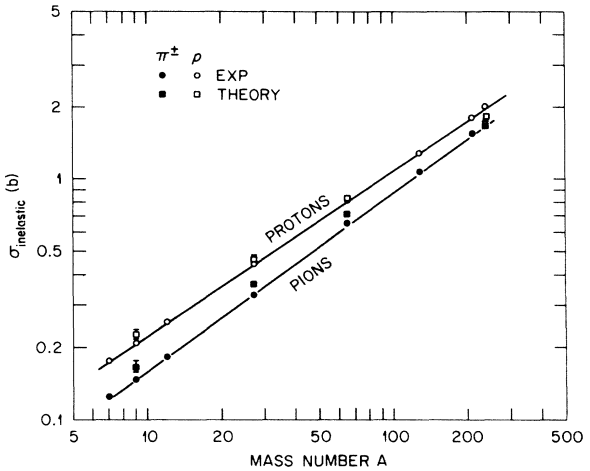

FIG. 8. Experimental and theoretical total inelastic cross sections for incident protons and pions on various nuclei. The experimental data are for incident 30–70-GeV $\pi^{\pm}$ and protons [S. P. Denisov *et al.*, Nucl. Phys. B61, 62 (1973), quoted by Busza, Ref. 5]. The calculated results are for incident 50-GeV π^{+} and protons. Where not illustrated, the statistical errors on the calculated results are of the order of the size of the symbols. Solid lines were drawn through the experimental data merely to guide the eye.

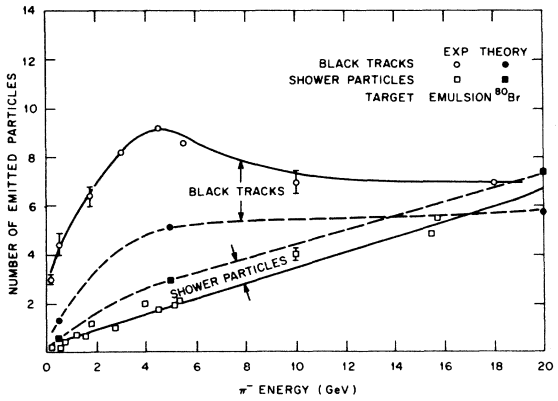

FIG. 9. Average number of shower particles and black tracks vs incident pion energy for π^- on emulsions. Experimental data quoted by V. S. Barshenkov, K. K. Gudima, and V. D. Toneev (Ref. 20). Theoretical results are from π^- on bromine-80. Solid and dashed lines are drawn through the experimental and theoretical data, respectively, merely to guide the eye. See text for details.

the calculation for incident π^- at various energies. The target used for the theoretical results was bromine-80 which was assumed to be representative of the constituents of the emulsion. The theoretical shower-particle data are taken to be the average numbers of π^+ and π^- produced with $\beta \geq 0.7$ (~56 MeV) per interaction, and the theoretical numbers representing black tracks are the sums of the average numbers of ^{1}H, ^{2}H, ^{3}H, ^{3}He, and ^{4}He that were evaporated following the cascade.

Even though they are fairly standard these theoretical assignments of shower particles and black tracks are somewhat arbitrary because the exact nature of the particles that are measured is ill-defined. Unfortunately, this lack of definition causes explanations of discrepancies between experimental results and theoretical predictions to be somewhat speculative in that the discrepancies may be partly due to a comparison of different entities rather than different values of the same entity.

Assuming that the theoretical assignments represent the quantities measured, the greatest discrepancies (~50%) between the predictions and the experimental data occur at about 4 GeV or lower for both the black tracks and the shower particles. At the highest energies the discrepancies are about 15%. The agreement of the theoretical results with the experimental data may be considered to be fair or poor.

However, at this stage of the development of the theoretical model the predicted trends in the energy dependence of the results in comparison with the experimental trends are about as important as

TABLE I. Theoretical values for the sum of π^+ and π^- with $\beta \geq 0.7$ emitted per interaction for incident protons.

Incident proton energy[a] (GeV or GeV/c)	Target p[b]	Target Br
10	0.70	3.8±0.1
100	1.88	14.2±0.3
1000	5.50	41.0±0.7

[a] For p-p interactions the units are GeV/c. For reactions with the complex nuclei, the units are GeV.

[b] These are the values obtained by taking $\frac{2}{3}$ of the results when Eq. (2) is integrated over angle and over secondary pion momenta.

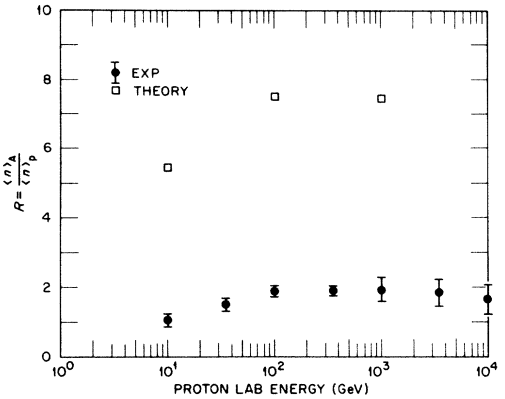

FIG. 10. Ratio of the number of shower particles produced by protons on emulsion to those produced by p-p collisions vs incident proton energy. Experimental data quoted by W. Busza (Ref. 5, p. 211). The statistical errors associated with the theoretical results are about the size of the symbols. See text for details.

the comparisons of the absolute values themselves. In this regard, the predicted trends are in excellent agreement with the experimental data. Since it is generally assumed that the black tracks are largely the result of the evaporation mechanism, and the number of black tracks is dependent on the excitation energy of the evaporating nucleus, both the experimental data and the theoretical predictions indicate the onset of a saturation effect for the excitation energy at about the same incident particle energy.

Relative multiplicities

A comparison between the experimental data[5] and the theoretical predictions for the ratio of shower particles produced in emulsions to those produced in p-p collisions vs incident proton energy is shown in Fig. 10. The experimental shower-particle data at incident particle energies greater than 300 GeV are from cosmic rays. The theoretical data are for incident protons on bromine-80, and the theoretical shower particles are as described in the previous section. The predicted ratios are high by factors of 4 and 5. Table I contains the theoretical results from which the data in Fig. 10 were obtained.

Similar discrepancies appear when the ratio is plotted vs mass number, as is illustrated in Fig. 11. The theoretical results are from 100-GeV π^- on C, Cu, and Pb, and the experimental data are the average values from 100- and 175-GeV incident π^- on the elements shown and for shower particles with $\beta \geq 0.85$ (~125-MeV pions).[21] Table II shows the data before the ratios were calculated where it is apparent that the theoretical model used to represent the reactions with protons underestimates the multiplicities by more than a factor of 3. In spite of this, the predicted multiplicities from reactions with nuclei are larger than the experimental values by 25 to 60%.

The implications from these comparisons are that the theoretical nuclear reaction model enhances the shower-particle production by the factors illustrated in Figs. 10 and 11. However, it does not necessarily follow that the same enhancement would be maintained if a more realistic pion-nucleon model were employed, and the reason is that if three times more particles (for example) are created in the initial collision with a nucleon

TABLE II. Theoretical and experimental (Ref. 21) shower-particle multiplicities from reactions of π^- on nuclei.

Incident pion energy	P Exp.	P Theor.[a]	C Exp.[b]	C Theor.	Cu Exp.[b]	Cu Theor.	Pb Exp.[b]	Pb Theor.
100	6.5±0.4	1.88	8.4±0.7	10.4±0.1	10.6±0.9	14.7±0.1	12.6±1.1	20.1±0.3
175	7.7±0.5							

[a] See footnote b, Table I.

[b] Results shown are the average values from 100- and 175-GeV incident π^-. These data were calculated from the values given in column 2 and those shown in Fig. 11, all of which were taken from Ref. 21.

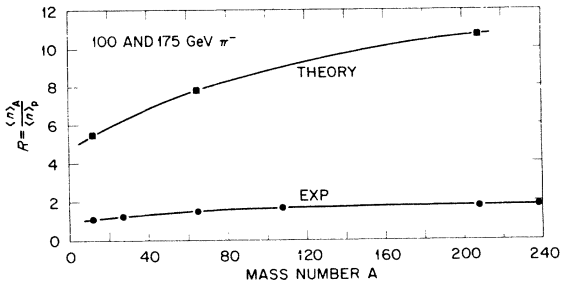

FIG. 11. Ratio of number of shower particles produced for various targets to those produced for a proton target. Experimental data are the average values from 100- and 175-GeV incident π^-, and the error bars are smaller than the symbols. (See Ref. 21.) Theoretical results are for incident π^- at 100 GeV, and the statistical errors are about the size of the symbols. Solid line curves are drawn through the experimental and theoretical data merely to guide the eye.

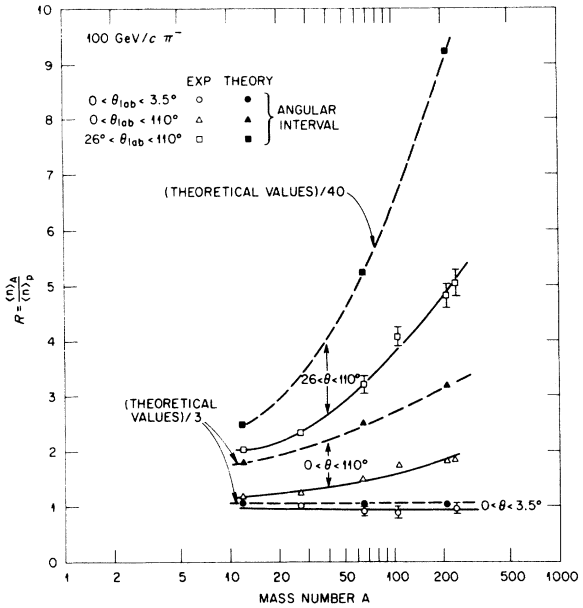

FIG. 12. Ratio of shower particles produced in various angular intervals from 100-GeV/c π^- on nuclei to those produced from 100-GeV/c π^- on p. The solid and dashed lines are drawn through the experimental and theoretical data, respectively, merely to guide the eye. $\beta > 0.85$ for the experimental data and ≥ 0.7 for the theoretical results. The theoretical values from the model have been divided by the values indicated. The statistical errors on the theoretical results are of the order of the size of the symbols.

inside the nucleus the average energy of these particles will be about a factor of 3 less. On subsequent collisions inside the nucleus these particles will create fewer particles than is presently the case. Verification of this thesis must await the implementation of a more realistic particle-nucleon model into the calculation, but such implementation will require a substantial effort.

As with the comparisons in the previous section, the important energy dependence of the results from the model, shown in Fig. 10, is in excellent agreement with that demonstrated by the experimental results, i.e., the theoretical model achieves a "saturation effect" of the shower-particle multiplicity at about the same energy as do the actual reactions. The predicted mass dependence of the multiplicity, Fig. 11, varies by about a factor of 2 from C to Pb while it varies by about 1.5 over the same mass range for the experimental data.

As pointed out by Busza, the most striking feature of the experimental data, both from counters and emulsions, is that the increase in the multiplicity with nuclear mass number occurs entirely at large angles.[5] There is no discernible enhancement of the multiplication in the forward direction with mass number. The theoretical results for various angular intervals are shown in Table III. There is no increase in the multiplicity over the mass range from C to Pb in the angular interval 0–3.5°, while there is a successively larger increase as larger angles are considered. For the data shown, the largest increase is for the angular interval 26–110°, hence the "striking" feature of the experimental data is predicted by the model. These angular intervals were selected to conform to those used in recent experiments.[21] Direct comparison with experimental data is somewhat difficult because these data were reported only in the form of ratios of multiplicities from nuclei to

TABLE III. Theoretical values of the sum of the numbers of π^+ and π^- with $\beta \geq 0.7$ produced in various laboratory angular intervals from 100-GeV incident π^-.

Lab angular interval	Target C	Cu	Pb	p
0–3.5°	3.37 ± 0.05	3.29 ± 0.05	3.15 ± 0.10	0.99
0–26°	8.15 ± 0.11	9.99 ±0.13	11.73 ± 0.27	1.86
0–110°	10.13 ± 0.15	14.18 ± 0.18	19.09 ± 0.45	1.88
26–110°	1.98 ± 0.04	4.19 ± 0.08	7.36 ± 0.20	0.02

those from protons, and, as discussed above, the theoretical model predicts these ratios to be large. Compounding the difficulty is the fact that the theoretical model representing the reactions with nucleons yields only ~1% of the total multiplicity in the last angular interval (26–110°) and, as a result, the theoretical ratios calculated for this angular interval, where the 1% value is used in the denominator, are very large. An attempt to compare the predicted ratios with the experimental data is shown in Fig. 12 where all of the theoretical ratios for the angular intervals 0–3.5° and 0–110° were arbitrarily divided by 3 and plotted, whereas the theoretical ratios for the angular interval 26–110° were divided by 40 before plotting.

Spectra

The spectra of secondary pions and protons at 13° and 45° from 33-GeV p on Al are shown in Figs. 13 and 14. The experimental data are not in absolute units but in units of particles/(sr GeV c) per circulating proton.[22] All of the theoretical results, calculated in units of mb/(sr GeV c), were arbitrarily divided by 2.5 for normalization purposes. The slopes of the pion and proton spectra, the relative magnitudes of pions to protons, and the change of these magnitudes with angle are fairly well represented by the theoretical predictions.

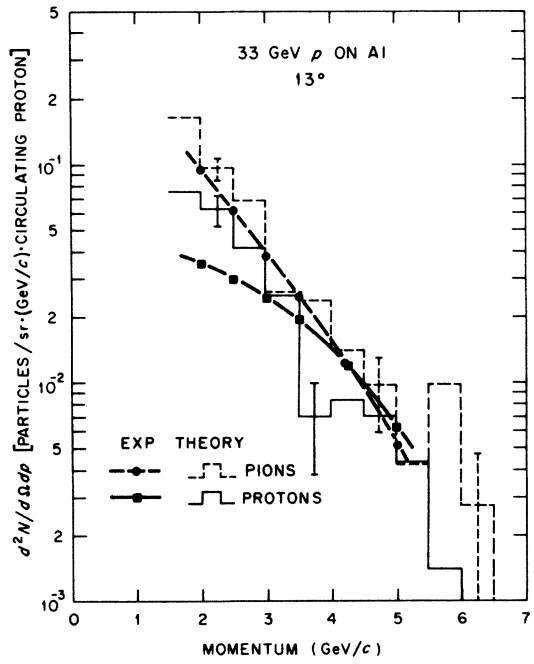

FIG. 13. Momentum spectra of pions and protons at a laboratory angle of 13° from 33-GeV p on Al. The experimental pion data represent either π^+ or π^- (their spectra are indistinguishable) and the experimental error bars for the pion and proton data are smaller than the symbols. The theoretical data are for π^+ and protons emitted into the angular interval 10–15°. Only representative statistical error bars are shown. The theoretical results, calculated in units of mb/(sr GeV c), have been arbitrarily divided by 2.5 for normalization purposes and plotted as shown.

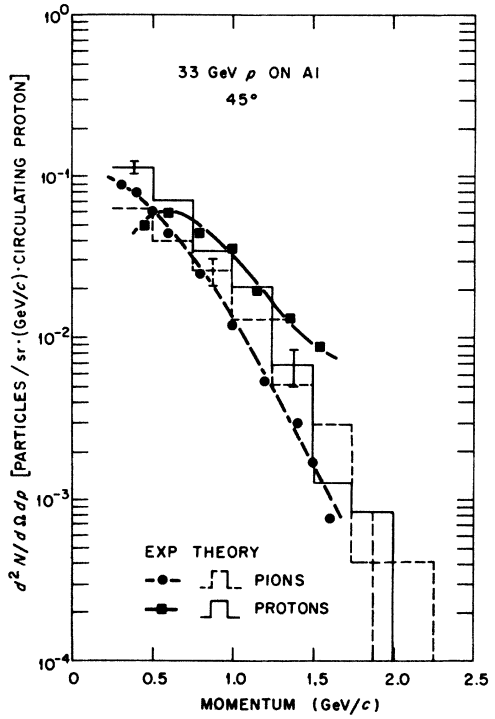

FIG. 14. Momentum spectra of pions and protons at a laboratory angle of 45° from 33-GeV p on Al. The theoretical results are for π^- and protons emitted into the angular interval 40–50°. Other details as in Fig. 13.

Radionuclides

The radionuclides produced from relatively low-energy (11.5 GeV) protons interacting with cobalt were measured and compared with those produced from high-energy protons (200 and 300 GeV), and it was found that the cross sections are essentially constant above 11.5 GeV.[23] Similar results were observed for silver[24] and uranium[25] targets. These results are consistent with those discussed above where the number of black tracks were shown to become independent of energy above ~5 GeV, and they are indicative of a saturation effect of the excitation energy of the residual nucleus.

Calculations were performed for 11.5- and 300-GeV p on cobalt, and the results were compared with the experimental data of Katcoff *et al.*[23] The theoretical and experimental data are shown in

TABLE IV. Theoretical and experimental (Ref. 23) cross sections for producing radionuclides from 11.5-GeV p on ^{59}Co, and also ratios of cross sections from 300-GeV p on ^{59}Co to those from 11.5-GeV p ($\sigma_{300}/\sigma_{11.5}$).

Nuclide	Mass No.	$\sigma_{11.5}$ (mb) Theor.	$\sigma_{11.5}$ (mb) Exp.	$(\sigma_{300}/\sigma_{11.5})$[a] Theor.	$(\sigma_{300}/\sigma_{11.5})$[a] Exp.
Co	58	49.8 ± 5.8	43 ± 3	0.8 ± 0.1	1.13 ± 0.10
	57	16.1 ± 3.3	20 ± 2	0.9 ± 0.3	1.10 ± 0.12
	56	4.9 ± 1.9	5.1 ± 0.4	0.7 ± 0.4	1.04 ± 0.10
	55	0.7 ± 0.7	0.66 ± 0.10	···	1.02 ± 0.17
Mn	54	10.5 ± 2.7	19 ± 2	0.9 ± 0.3	1.06 ± 0.12
	52	7.0 ± 2.0	5.4 ± 0.5	0.6 ± 0.3	1.04 ± 0.12
Cr	51	10.5 ± 2.7	21 ± 2	0.8 ± 0.3	1.01 ± 0.11
	48	1.4 ± 1.0	0.28 ± 0.02	0.5 ± 0.5	0.93 ± 0.08
V	48	9.1 ± 2.5	9.4 ± 0.7	0.6 ± 0.3	1.00 ± 0.09
Sc	48	0.0	0.60 ± 0.07	···	0.95 ± 0.12
	47	0.7 ± 0.7	2.7 ± 0.2	1.0 ± 1.0	1.05 ± 0.09
	46	3.5 ± 1.6	6.7 ± 0.5	1.0 ± 0.6	1.01 ± 0.09
	44	8.4 ± 2.4	4.8 ± 0.3	0.8 ± 0.3	1.03 ± 0.10
K	43	0.7 ± 0.7	1.28 ± 0.11	1.0 ± 1.0	0.98 ± 0.13
	42	2.8 ± 1.4	3.9 ± 0.5	0.5 ± 0.4	0.85 ± 0.12
Mg	28	0.0	0.51 ± 0.04	···	1.06 ± 0.11
Na	24	1.4 ± 1.0	4.43 ± 0.25	1.5 ± 1.4	1.02 ± 0.09
Be	7	0.0	10.2 ± 1.1	···	1.15 ± 0.17

[a] Theoretical ratio is left blank if either σ_{300} or $\sigma_{11.5}$ are zero.

Table IV. The agreement is reasonable for the cross sections from the interactions at 11.5 GeV, and essentially all of the ratios of the cross sections from the interaction at 300 GeV to those at 11.5 GeV are within the statistics of the experimental ratios. The saturation effect for the excitation energy is thus well reproduced by the theoretical model.

The absolute values of the experimental cross sections were evaluated under the assumption that the cross section for the monitor reaction, ^{27}Al(p, $3pn$)^{24}Na, remained constant at 8.6 mb over the energy range of the experiments.[23] The calculated values for this cross section from the model were 7.7 ± 2.0 mb at 11.5 GeV and 8.7 ± 2.1 mb at 300 GeV, and hence no renormalization was necessary for these comparisons.

SUMMARY

An intranuclear cascade model for reactions of pions and nucleons with complex nuclei that should cover the energy range from ~50 MeV to ~1000 GeV has been developed. The model includes the effect of a diffuse nuclear surface, the Fermi motion of the bound nucleons within the nucleus, the exclusion principle, a local potential for nucleons, a localized reduction of the density of the nucleus during the development of the cascade, and the sequencing of the cascade events correct with time. Since the model yields essentially the same results as earlier versions at low energy[3,4,10] (≲3 GeV), comparisons were made with experimental data only at the higher energies to validate the model.

At energies ~50 GeV the absolute value and the mass dependence of the reaction cross section for incident protons and pions calculated from the model are in good agreement with experimental data.

Over the energy range from ~1–20 GeV, the predicted number of black tracks and the number of shower particles from pions on emulsion nuclei differs from experimental data by about a factor of 2 and ~50%, respectively, at 5 GeV, but these differences decrease to about 15% for both types of tracks at 20 GeV. The energy dependences of the multiplicities of both track types are in good agreement with the experimental results, particularly in that the number of black tracks produced becomes independent of energy above 5 GeV.

The absolute value of the predicted shower-particle multiplicities for 100-GeV pions on various nuclei is greater than the measured value by about 25% for light nuclei and greater by about 60% for heavy nuclei. The ratios of these multiplicities to those from protons are greater than the experimental ratios by factors of 4 or 5. This results

TABLE V. Running times for HECC-1 on the IBM 360/91 for various cases.

Incident particle energy (GeV)	Cascade cutoff energy	Target	Minutes/(1000 incident particles)
100	0.056	C	7
11.5	0.0	Al	9
50	49	Al	0.5
300	0.0	Al	28
5	0.0	Br	15
5	0.056	Br	10
20	0.0	Br	29
20	0.056	Br	21
100	0.056	Br	48
1000	0.056	Br	110
100	0.056	Pb	102
200	0.056	Pb	150

from the fact that the theoretical particle-proton model underestimates the number of shower particles produced per interaction. Replacing this model with a more realistic version will require considerable effort, but such a replacement, along with other modifications to improve the overall calculation, will be undertaken in the future. The effect of the inclusion of a more realistic particle-proton model is not clear. The calculated ratios of shower particles from nuclei to those from protons for 100-GeV incident pions vary by about a factor of 2 from carbon to lead whereas the experimental data show a variation of about 1.5 over the same mass range.

The energy dependence of these ratios for 10- to 1000-GeV protons on emulsions is well represented by the theoretical results.

A salient feature of the experimental data is that the shower-particle multiplicity in the forward direction is independent of target mass. The increase in the multiplicity with mass occurs mainly at large angles. This feature is fairly well reproduced by the theoretical model.

The agreement in absolute value between the theoretical predictions and the experimental data of the radionuclides produced from 11.5- and 300-GeV p on cobalt is reasonable. More important is that the calculation predicts a relatively constant value for these cross sections over the energy range considered, which is in agreement with the experimental observations.

In short, the model overestimates the shower-particle multiplicities by about 25% for high-energy reactions with light nuclei, and by about 60% for heavy nuclei. All other mass-dependent and energy-dependent trends that were investigated are predicted reasonably well.

COMPUTER CODE INFORMATION

The code HECC-1 (high-energy cascade code, version 1) occupies 1 210 000 bytes in the IBM 360/91 computer. The running times for typical cases are given in Table V. Note that these times are very sensitive to the cascade cutoff energy, i.e., the energy below which cascade histories are no longer followed.

*Research sponsored by the Department of Energy under contract with the Union Carbide Corporation.

†Neutron Physics Division.

‡Computer Sciences Division.

[1]N. Metropolis, R. Bivins, M. Storm, A. Turkevich, and G. Friedlander, Phys. Rev. 110, 185 (1958); N. Metropolis, R. Bivens, M. Storm, J. M. Miller, G. Friedlander, and A. Turkevich, Phys. Rev. 110, 204 (1958).

[2]M. P. Guthrie, ORNL Report No. ORNL/TM-3119, 1970 (unpublished). The basis of this model is that of I. Dostrovsky, Z. Fraenkel, and G. Friedlander, Phys. Rev. 116, 683 (1959).

[3]H. W. Bertini, Phys. Rev. 188, 1711 (1969).

[4]H. W. Bertini, Phys. Rev. C 6, 631 (1972).

[5]W. Busza, in *High-Energy Physics and Nuclear Structure—1975*, edited by H. C. Wolfe (American Institute of Physics, New York, 1975), conference proceedings No. 26, p. 211–236.

[6]L. Bertocci, in *High Energy Physics and Nuclear Structure—1975* (see Ref. 5), p. 238.

[7]K. Gottfried, Phys. Rev. Lett. 32, 957 (1974).

[8]M. Miescowicz, in *Progress in Elementary Particle and Cosmic Ray Physics*, edited by J. G. Wilson and A. Wouthuysen (American Elsevier, New York, 1971), Vol. X, p. 65; A. Z. Patashinskii Zh. Eksp. Teor. Fiz.-Pis'ma Red. 19, 654 (1974) [JETP Lett. 19, 338 (1974)].

[9]I. Z. Artykov, V. S. Barashenkov, and S. M. Eliseev, Nucl. Phys. 87, 241 (1966); I. Z. Artykov, V. A. Barashenkov, and S. M. Eliseev, JINR Report No. JINR-P2-3604, 1967 (unpublished); V. S. Barashenkov, K. K. Gudima, and V. D. Toneev, Acta Phys. Pol. 36, 887 (1969).

[10]H. W. Bertini, Phys. Rev. 131, 1801 (1963).
[11]K. Chen *et al.*, Phys. Rev. 166, 949 (1968).
[12]K. Chen *et al.*, Phys. Rev. C 4, 2234 (1971).
[13]N. B. Gove *et al.*, Oak Ridge National Laboratory Report No. ORNL/Tm-2627, 1969 (unpublished). The numerical approach was employed, p. 25. The momentum range 0-p_{Fermi} and the angular range $-1 \leq \mu \leq 1$ ($\mu = \cos\theta$) were divided into 10 uniform intervals each.
[14]B. G. Gibbard *et al.*, Phys. Rev. Lett. 24, 22 (1970).
[15]D. Harting *et al.*, Nuovo Cimento 38, 60 (1965).
[16]H. W. Bertini *et al.*, Oak Ridge National Laboratory Report No. ORNL/TM-5710, 1977 (unpublished).
[17]R. M. Sternheimer and S. J. Lindenbaum, Phys. Rev. 123, 333 (1961): 109, 1723 (1958); 105, 1874 (1957).
[18]J. Ranft, Nucl. Instrum. and Methods 48, 133 (1967).
[19]J. Ranft, CERN Report Nos. MPS/Int. MU/EP 66-3, and JR/id 9.2., 1966 (unpublished).
[20]V. S. Barashenkov, K. K. Gudima, and V. D. Toneev, Acta Phys. Pol. 36, 457 (1969).
[21]W. Busza *et al.*, Phys. Rev. Lett. 34, 836 (1975).
[22]V. L. Fitch, S. L. Meyer, and P. A. Piroué, Phys. Rev. 126, 1849 (1962).
[23]S. Katcoff *et al.*, Phys. Rev. Lett. 30, 1221 (1973).
[24]G. English, Y. W. Yu, and N. T. Porile, Phys. Rev. Lett. 31, 244 (1973).
[25]S. K. Chang and N. Sugarman, Phys. Rev. C 9, 1138 (1974).